Photoinduced Chemical Vapor Deposition of Amorphous Carbon Films from Chloromethane Using a VUV Laser (157 nm)

Terttu I. Hukka*,† and Jie Zhang‡

Institute of Materials Chemistry, Tampere University of Technology, P.O. Box 541, 33101 Tampere, Finland, and Department of Electrical and Computer Engineering, University of Toronto, 10 King's College Road, Toronto, Ontario, Canada

Received: December 20, 1999; In Final Form: May 9, 2000

Amorphous carbon (*a*-C) films with low hydrogen content were deposited at low substrate temperatures from a chlorinated hydrocarbon (CH_3Cl) by photoinduced chemical vapor deposition with a fluorine laser (157 nm). The optical gap, as determined by photothermal deflection spectroscopy (PDS), decreased from 2.3 to 0.1 eV when the substrate temperature was increased from 303 to 643 K. The films were further characterized by FTIR spectroscopy, micro-Raman spectroscopy, surface acoustic wave spectroscopy (SAWS), and atomic force microscopy (AFM). The presence of chlorine residues in the films was examined by energy-dispersive X-ray fluorescence (EDXRF) spectroscopy. The amount of chlorine decreased significantly between 493 and 518 K, causing the carbon network to restructure into a more graphitic form. Deposition at 643 K produced a chlorine-free *a*-C film on the quartz substrate.

1. Introduction

Deposition of amorphous carbon (*a*-C) films from hydrocarbon sources and graphite has been extensively studied during the past decade because of the interest in producing thin films for a variety of applications for which diamond-like optical, electronic, chemical, and mechanical properties are desired. Developing an understanding and control of the growth process producing amorphous carbon thin films has been much more difficult than for that of other amorphous semiconductors, but continuous progress has been made. Various ion beam techniques and conventional chemical vapor deposition (CVD) methods have been used to grow interconnected carbon networks with high mass densities and high sp^3/sp^2 carbon ratios.[1] Halogen-assisted growth of diamond[2,3] has been investigated and demonstrated under CVD conditions; however, only a few studies have been reported on the growth of amorphous carbon films from halogenated hydrocarbon precursors using a laser-assisted chemical vapor deposition method.[4−7] Not much is known, therefore, about the relationship between the physical properties of the deposited *a*-C films and the deposition conditions of the laser-induced growth process in general and about the laser-induced growth processes involving halogenated hydrocarbons in particular.

One disadvantage of conventional CVD methods for *a*-C deposition in which methane or other hydrocarbons are used as precursors is that thin films with high hydrogen content are typically produced. The high H content reduces the amount of C−C sp^3 bonding and, thereby, the diamond-like character of the amorphous carbon films. High fractions (75−95%) of sp^3 bonding have been determined in films grown by pulsed laser deposition.[8] The pulsed-laser method accordingly would seem to be a good choice for producing *a*-C and diamond-like carbon (DLC) films with low hydrogen concentrations and high degrees of sp^3 bonding.

The laser methods allow deposition of non-hydrogenated DLC films at lower substrate temperatures than the plasma-assisted chemical vapor deposition or sputtering methods because the precursor is decomposed photolytically. Moreover, because a C−Cl bond is weaker than a C−H bond, the decomposition of the chlorinated hydrocarbon precursors is energetically more favorable than the decomposition of halogen-free hydrocarbons, such as methane. This enables lower substrate temperatures even for conventional methods. Laser techniques are also capable of producing very smooth *a*-C films, typically on a nanometer scale.

The purpose of this work is to improve our understanding of the relationship between the physical properties of amorphous carbon films and the deposition conditions under photoassisted CVD. Chloromethane was used as the halogenated hydrocarbon precursor. The structural and mechanical properties of the films were determined using a set of complementary methods.

2. Experimental Section

2.1. Deposition. The experimental setup used for the photodeposition of *a*-C:H,Cl has been explained elsewhere[9] and is described here only briefly. The photoinduced decomposition of the reactant gas molecules was carried out using a Lambda Physik LPF 205 fluorine laser in a parallel configuration with respect to the substrates. The average laser output power was 3.0 W at 157 nm. The laser was operated at a repetition rate of 50 Hz, with pulse energies up to 80 mJ. Two different beam configurations were used: unfocused (5×13 mm^2) and focused (5×5 mm^2). A cylindrical planoconvex MgF_2 lens (25×25 mm^2, VUV quality, coated for 157 nm) with a focal length of 500 mm, located in front of the substrate holder, was used for focusing. The laser beam was directed through a MgF_2 window into a stainless steel deposition chamber ($V = 14$ dm^3) with a base pressure of 10^{-7} mbar. The distance of the substrate surface

* Author to whom correspondence should be addressed. Telephone: +358−3−365 3632. Fax: +358−3−365 2108. E-mail: terttu.hukka@cc.tut.fi.

† Tampere University of Technology.

‡ University of Toronto.

10.1021/jp994452d CCC: $19.00
Published on Web 07/06/2000

TABLE 1: Properties of the Deposited *a*-C Films

sample	T (K)	d (mm)	p_{CH3Cl} (μbar)	p_{tot} (mbar)	film thickness (nm)[a]	growth rate (nm/min)[a]	RMS (nm)[a]	E_g (eV)	E_{o4} (eV)	E_o (meV)	ρ (g/cm^3)[a]	elastic modulus (GPa)[a]	laser P/E (W/mJ)
1	303	5	53	2	500, 700	1.5, 2.1	0.33, 0.54	2.3	>2.8	240	2.9, 2.1	15, 40	−
2	303	5	22	1	400−600[b]	1.0−1.7[b]	0.55−0.86	2.2	2.8	244	3.3[b]	55[b]	2.5/50
3	353	5	53	2	200, 350	1.4, 2.5	0.28, 0.69	2.0	2.5	251	−	−	−/60
4	423	5−8	53	2	150, 200	0.6, 1.2	0.30	1.6	2.0	278	−	−	−/60
5	493	1−2	20	1	200, 400	1.0, 2.1	0.37, 1.74	1.0	1.8	473	2.2, 2.4	50	2.7/55
6	518	1−2	20	1	300	0.9	0.69, 3.09	0.6	−	585	−	−	3.2/65
7	523	5	53	2	350, 500	0.9, 1.4	0.84, 0.55	0.5	1.1	590	1.4[c]	50[c]	−/55
8	573	5	53	2	200, 350	0.7, 1.2	0.85, 1.73	0.5	0.8	640	−	−	−
9	573	1−2	20	1	225, 600[d]	1.1, 3.0	0.84, 4.23	0.4	<0.6	1477	2.2−2.3[c]	180−200[c]	4.0/80
10	593	1−2	20	1	200[e]	0.7[e]	0.67, >25	0.1	<0.6	1478	2.0	50	3.0/60
11	573	1−2[f]	20	1	175, 500	0.7, 2.0	0.47, 4.04	0.2	<0.6	1791	−	−	3.8/77
12	593	1−2[f]	20	1	55, 40	0.2[e]	0.49, 1.67	0.2	<0.6	∞	−	−	2.7/53
13	623	5−10	25	1	40	0.4	1.0	0.1	−	∞	−	−	−/60
14	643	1−2	20	1	180−1000[b]	0.7−4.0	0.67	0.1	<0.6	1223	−	−	3.0/60
14	643	1−2	20	1	150	0.6	>100	−	−	−	−	−	3.0/60

[a] First figure is for the film on a quartz substrate, and the second for the film on a silicon substrate, unless otherwise mentioned. [b] On a quartz substrate. [c] On a silicon substrate. [d] SAWS measurement yields a film thickness of 530−730 nm. [e] On both substrates. [f] Focused laser beam has been used.

from the laser beam was set to either 1−2 or ca. 5 mm. No deposition was detected when the beam was touching the substrate surface.

Chloromethane (CH_3Cl, 99.8 vol % from Messer Griesheim) was used as the reactant gas. Chloromethane has an absorption cross section of ca. 10 Mb at a wavelength of 157 nm.[10] Energetically, the most probable dissociation products of CH_3-Cl are CH_3 and Cl photofragments (3.5 eV, 3.6 eV for Cl*).[11] Dissociation to CH_2Cl and H species is also probable although the process consumes slightly more energy (3.9 eV) because of the slightly stronger C−H bond. The reactant gas entered the deposition chamber through a 4-mm inner diameter stainless steel tube at a distance of either 15 mm (at 573 K) or 25 mm (in all other experiments) above the substrate surface. The distance of the reactant gas doser from the middle of the laser beam was kept constant. The flow of chloromethane gas was adjusted to either 2 or 5 sccm using a mass flow controller. Helium gas (99.9999 vol %) was used as a buffer gas at a flow rate of 100 sccm. Deposition at the laser entrance window, which was located at a separated baffle, was reduced by flushing the window with the buffer gas before it entered the deposition chamber. Flushing allowed for photodeposition of several hours. The total gas pressure and the substrate temperature were kept constant during each deposition. Either 1 or 2 mbar was chosen for the total gas pressure, and the substrate temperature was varied between 303 and 643 K.

Quartz plates (Heraeus Quartzglass, Quality He 1, 3 × 20 × 30 mm^3) and 200-μm-thick intrinsic or 2-mm-thick slightly n-doped (resistance ca. 5000 Ω cm) silicon (111) plates were used as substrate materials.

2.2. Analytical Methods. The surface morphology of the films was studied by atomic force microscopy (AFM) using a Topometrix TMX 1010 Explorer atomic force microscope, which operates under ambient atmosphere. Optical absorption spectra were measured by photothermal deflection spectroscopy (PDS)[12] in the region of 0.5−2.8 eV. Density and Young's modulus were determined by surface acoustic wave spectroscopy (SAWS) on continuous films with a thickness of >400 nm.[12]

A Bruker IFS 66v vacuum Fourier Transform infrared (FTIR) spectrometer with a DTGS detector was used to obtain information on the hydrogen, chlorine, and carbon bonding in the films. The recorded spectral region was 500−4000 cm^{-1}. Resolution was 8 cm^{-1}.

The graphitic features of the amorphous carbon films were investigated by Raman spectroscopy. The spectra were recorded with a Dilor Labram1 micro-Raman spectrometer with an argon laser (514.5 nm). Laser beam intensities were 5 and 15 mW, and collecting times were 3 and 1 s, respectively. The spectrometer was equipped with a CCD camera connected to an optical microscope. The image size was 58 × 80 μm^2.

Each substrate was partially covered with a ceramic plate during the deposition in order to create an edge over which the film thickness was recorded with a Talystep stylus profilometer (Rank Taylor Hobson Ltd.).

The relative amounts of chlorine in the deposited films were determined by energy-dispersive X-ray fluorescence spectroscopy (EDXRFS). The measurements were carried out with an ACAX 300 EDXRF spectrometer equipped with a solid-state Si(Li) detector and a microcomputer for handling the data and controlling the instrument. The sample was excited with an annular Fe-55 100mCi (5.89 keV) radioisotope source, and the XRF spectra were measured in 2048 microchannels.

3. Results and Discussion

3.1. Deposition. The rate of deposition of the amorphous carbon films from CH_3Cl was relatively low and may have affected the structure of the films. The total deposition time was 4−6 h. During each deposition, the gas laser was filled 4−5 times, and each filling took 10−15 min. During filling, the flow of the process gas into the chamber was stopped, but the substrate temperature was kept constant. This means that, during the filling, the film was annealed at the deposition temperature. It may be possible that, at the highest annealing temperatures, diffusion and desorption of atoms (Cl, H) changed the film network toward a more graphitic structure.

3.2. Density and Young's Modulus. The densities and Young's moduli were determined by SAW spectroscopy for carbon films with thicknesses greater than 400 nm. The results are given in Table 1. The Young's modulus is not a direct measure of the material hardness but gives relative information about the hardness in comparison with the Young's moduli of other materials. Evidently, the laser power affects the elastic properties, and accordingly the hardness, of the deposited films. Specifically, the highest value of Young's modulus of 180−200 GPa (see Table 1) was measured for the film deposited at 573 K on a silicon substrate with the highest obtainable laser power and energy (4.0 W and 80 mJ). The measured value is

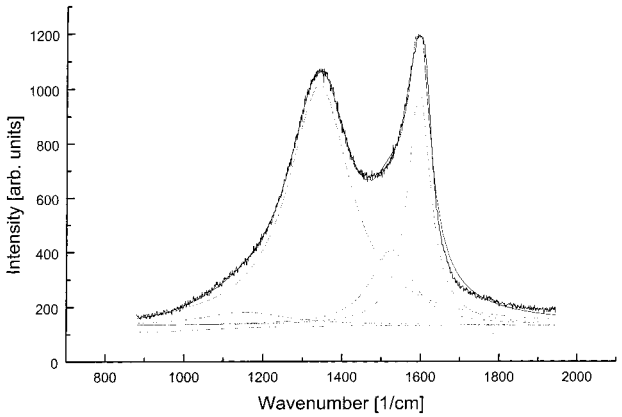

Figure 1. Raman spectrum of the *a*-C film deposited at 573 K on a quartz substrate.

TABLE 2: Peak Positions of the Nondeconvoluted Raman Spectra

sample	*T* (K)	*P* (mW)	D-band (cm^{-1})[a]	D-band (cm^{-1})[b]	G-band (cm^{-1})[a]	G-band (cm^{-1})[b]
5	493	5	−	1344	−	1593
6	518	5	−	1340	−	1598
7	523	5	1344	1340	1592	1593
9	573	15	1336	1345	1597	1591
10	593	15	1340	1344	1592	1593
11	573[c]	15	1337	1336	1605	1596
12	593[c]	15	1344	1338	1593	1593
14	643	15	1344	1344	1597	1593

[a] Film was deposited on a silicon substrate. [b] On a quartz substrate. [c] Focused laser beam was used during the deposition.

close to the Young's modulus of quartz (200 GPa) and somewhat lower than the value measured for amorphous carbon films produced by cathodic-arc deposition (400 GPa).[14] Young's moduli for polycrystalline diamond films are substantially larger, ca. 900−1100 GPa.[13]

The density of the film yielding the highest Young's modulus was 2.2−2.3 g/cm^3 (see Table 1), which is of the same order as those of graphite and quartz. Focusing of the laser beam produced soft films at 573 and 593 K.

3.3. Raman Measurements. Raman scattering spectra were collected for the films deposited at temperatures above 490 K. The films deposited below 490 K were relatively soft and became damaged during the photon bombardment of the micro-Raman spectrometer, even at low laser powers.

A Raman spectrum of the *a*-C film deposited on quartz at 573 K with a $CHCl_3$ partial pressure of 20 μbar is presented in Figure 1. The shape of the spectrum is typical of all of the Raman spectra measured. The disordered (D) and ordered (G) graphite bands dominate the spectra, as is typical for amorphous carbon structures.[15−18] On both silicon and quartz substrates (see Table 2), the centers of the maxima of the nondeconvoluted D bands are located between 1336 and 1345 cm^{-1}, and those of the G bands between 1591 and 1605 cm^{-1}. The peak positions of the nondeconvoluted spectra do not seem to depend on the deposition temperature within the range 490−640 K. The D peak is of higher intensity than the G peak. In addition, the intensity ratio of the D and G peaks varies only slightly above 518 K. These observations point to a high but relatively constant degree of sp^2 bonding in the films deposited at 520−640 K.

Deconvolution of the Raman spectra of films deposited on the quartz substrates at 523−593 K yielded two main bands, D and G, centered at 1338−1346 and 1592−1598 cm^{-1}, respectively, and two additional components centered at 1123−1168 and 1526−1556 cm^{-1}. The deconvolution of the Raman spectrum of the film deposited at 573 K is presented in Figure 1. The data points for the deconvolution were taken within the range of 880−2000 cm^{-1}.

When the substrate temperature is increased from 523 to 593 K, the deconvoluted D peak moves to slightly lower wavenumbers, and the width of the D peak decreases from 250 to 170 cm^{-1}. This is in accordance with the work of Sattel et al.,[18] who observed that the D peak of *ta*-C:H started to move from 1375 toward 1330 cm^{-1} and to become narrower when the deposition temperature was increased from about 500 to 523 K.

The position of the deconvoluted G peak (ca. 1595 cm^{-1}) remains approximately the same over the whole deposition temperature range. Also, the width of the G band remains relatively wide and constant (ca. 60 cm^{-1}) in the range 523−593 K. The width of the G peak is about the same as that observed for amorphous carbon (75 cm^{-1})[18] and comparable to that of glassy carbon (61−79 cm^{-1}).[19] Usually, when the amount of graphitic bonding increases, the G peak moves to higher wavenumbers, and the peak width decreases. Polycrystalline and pyrolytic graphite have peak widths of only about 28 and 23 cm^{-1}, respectively.[19] It seems clear, therefore, that the changes in the amount of graphitic bonding are relatively minor in this temperature range. At deposition temperatures lower than 523 K, where the concentration of the chlorine atoms is originally higher, one would expect more marked changes in the material characteristics, as observed in the PDS results discussed below. The width of the G peak suggests that there is disorder and stress in the deposited *a*-C films, which was confirmed by the PDS results (see below).

Our work suggests that, in the films deposited using photo-assisted decomposition of CH_3Cl, the transition temperature for the graphitization of the C−C bonds is about 518−523 K. Above this temperature, the concentration of the chlorine atoms starts to approach zero, which enables restructuring of the network. This finding is in accordance with the transition temperature of 523 K observed for plasma-deposited hydrogenated *ta*-C films.[18] Similarly, in the case of amorphous carbons deposited by cathodic arc or laser ablation, a sharp drop in the fraction of sp^3 bonding has been observed to take place at about 550 K.[20] A restructuring of the network from tetrahedral sp^3 to trigonal sp^2 and a simultaneous evolution of hydrogen have been reported in other studies in the slightly higher temperature range of 573−673 K.[18,21−23] Because the strengths of the C−H and the C−Cl bonds are similar, one would expect graphitization of the *a*-C:H, *a*-C:Cl, and *a*-C:H,Cl films, in which hydrogen and chlorine atoms are chemically bound to carbon atoms, to take place at more or less the same temperature.

Assignment of the peak appearing in the lowest wavenumber range (1120−1189 cm^{-1}) is not simple. The peak moves toward higher wavenumbers as the deposition temperature is increased (573−593 K). The width of the peak varies between 105 and 135 cm^{-1} when the data points are restricted to within 880−2000 cm^{-1} in the fitting. When the Raman spectrum of the hardest film deposited at 573 K was fit with all the available data points, the fitting yielded a peak centered at 1144 cm^{-1} with a fwhm of 82 cm^{-1}. This is very close to the peak at 1150 cm^{-1} (fwhm of 81 cm^{-1}) assigned to nanocrystalline diamond,[24,25] but, unfortunately, the assignment is still under discussion. The peak is also relatively close to a peak (1175 cm^{-1}) that has been assigned to sp^3 bonding due to microcrystalline or amorphous diamond.[26,27] Arguing against this, however, is the fact that tailing appears, with a maximum around

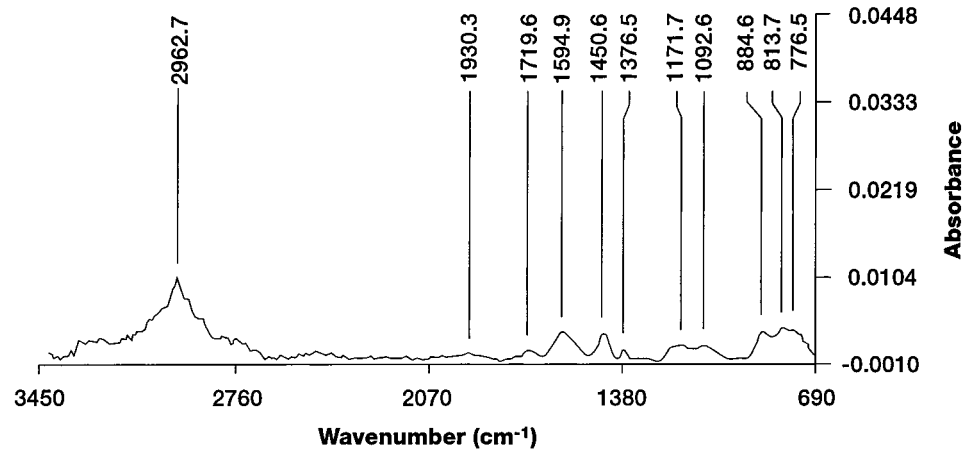

Figure 2. FTIR spectrum of a hydrogenated *a*-C film deposited at 523 K on a silicon substrate.

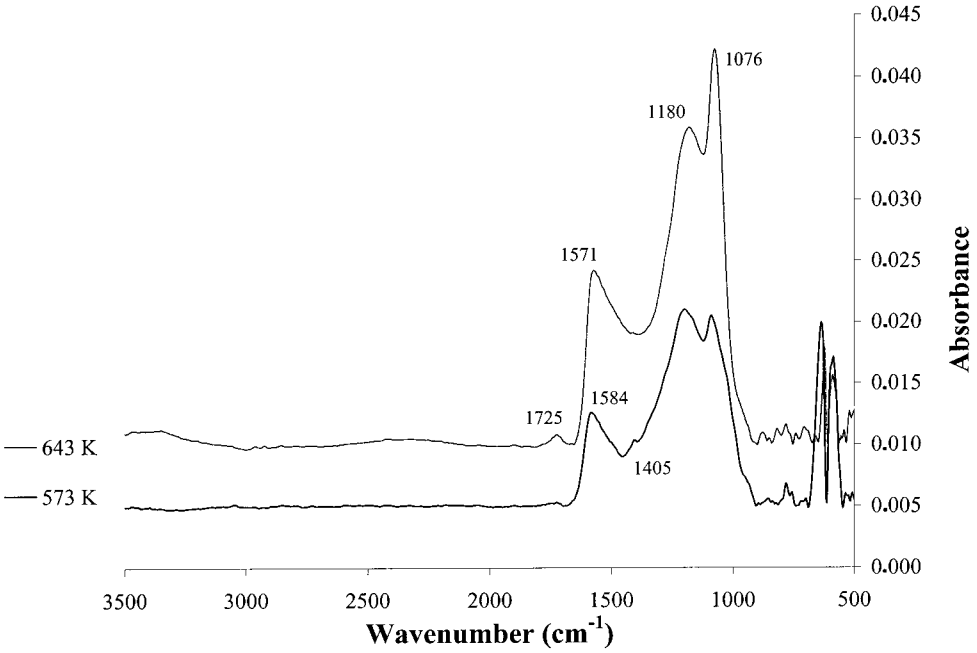

Figure 3. FTIR spectra of *a*-C films deposited at 573 and 643 K on silicon.

1150 cm^{-1}, in a Raman spectrum of charcoal.[19] Moreover, Fayette et al. have associated the band at 1150 cm^{-1} with the small grain size of the crystals constitutive of a film with amorphous phases.[28] Lee et al. have attributed the peak at 1138 cm^{-1} in spectra of their diamond films to small or defective sp^3-carbon nanocrystals.[29] Therefore, the origin of our peak at 1144 cm^{-1} remains unclear.

The origin of the additional component appearing around 1540 cm^{-1} after deconvolution of the Raman spectra of the films deposited on quartz is not unambiguous, either. When the substrate temperature is increased, the peak moves toward slightly lower wavenumbers, and the width of the peak increases from 110 to 125 cm^{-1} between 523 and 593 K. Although at the distinctly lower wavenumbers of 1467 and 1480 cm^{-1}, an additional component was found to be necessary to achieve optimum results in the deconvolution of the Raman spectra in the work of Gerber et al.[25] and Schwan et al.[27] Gerber et al. attributed their peak at 1467 cm^{-1} to a diamond precursor, but cautioned that the origin was not entirely clear. There are other possibilities for the band. Diamond-like carbon (DLC) films with a high degree of sp^2 bonding typically yield a Raman scattering band that is centered at 1515−1555 cm^{-1}.[19,20,23] In addition, carbon-rich SiC and SiC:H yield a Raman band at around 1500 cm^{-1}. The origin of the band at 1540 cm^{-1} remains unconfirmed, therefore.

3.4. FTIR Spectroscopy. An FTIR spectrum typical of the hydrogenated *a*-C films is shown in Figure 2. The film was deposited at 523 K on a 200-μm silicon substrate using a CH_3-Cl precursor partial pressure of 53 μbar. The film had a low elastic modulus of about 50 GPa.

Figure 3 shows the FTIR spectra of two amorphous carbon films deposited on a Si(111) substrate at higher temperatures of 573 and 643 K, using lower partial pressures (20 μbar) of CH_3Cl. These films have very low hydrogen concentrations. The film deposited at 573 K yielded the highest Young's modulus measured in this work, 180−200 GPa.

The amount of covalently bonded hydrogen was very low in all of the films grown at 20 μbar CH_3Cl partial pressure and temperatures above 490 K. The C−H stretching frequencies appearing at 2851 cm^{-1} (symmetric sp^3 CH_2), 2894 cm^{-1} (symmetric sp^3 CH_3), 2927 cm^{-1} (asymmetric sp^3 CH_2), and 2966 cm^{-1} (asymmetric sp^3 CH_3) were distinguished with a 10-fold magnification of the baseline of the FTIR spectrum recorded from the film deposited at 573 K. The wavenumbers are close to and the assignments correspond to those reported for CVD diamond[30,31] and *a*-C:H films.[32,33] The amount of unbound

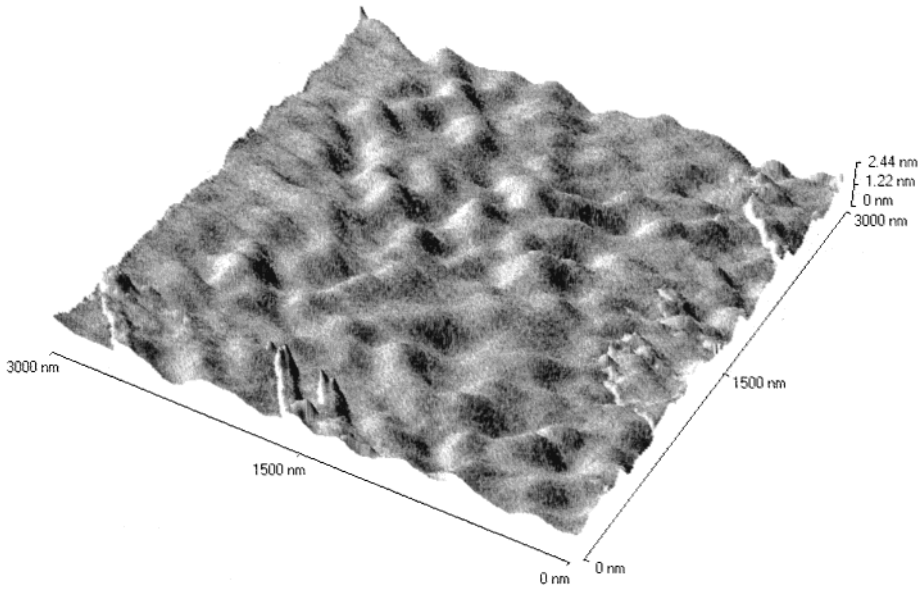

Figure 4. AFM image of a smooth *a*-C:H,Cl film deposited at 303 K on a quartz substrate.

hydrogen in our films is unknown, because the total hydrogen content of *a*-C:H films cannot be determined by FTIR.[34] The deformation peaks of sp^3 C−CH_3, typically occurring around 1370 and 1450 cm^{-1}, are clearly visible in the spectrum of the film deposited at 523 K with the higher CH_3Cl partial pressure (Figure 2). If present at all, the C−CH_3 vibrations are not, however, separated from the main peak in the spectra of the films grown using the lower CH_3Cl partial pressure and higher temperatures (Figure 3).[35]

The 1405 and 1584 cm^{-1} vibrations recorded for the film grown at 573 K (Figure 3) are assigned to the aromatic sp^2 C−C vibrations on the basis of assignments reported in the literature (1400−1430 cm^{-1} and 1570−1600 cm^{-1}, respectively).[32,35,36] The peaks around 1170−1200 and 1070−1090 cm^{-1} are found in the literature as fitting parameters for the FTIR spectra of *a*-C:H[37] and occur in the region of impurity-related O−H and C−O vibrations. These vibrations possibly originate from oxygen adsorbed in the form of water onto the hydrogen- and chlorine-deficient surfaces. At 643 K, O−H and C═O vibrations are also clearly visible around 3500 and 1720 cm^{-1}, respectively.

Hydrogen atoms bound to the sp^2 carbon atoms yield C−H vibrations around 880, 820, and 760 cm^{-1}.[35,36,38] These vibrations are clearly visible in the spectra of the films grown with higher precursor pressures, as shown in Figure 2, but are relatively weak in the spectra of the films grown at higher substrate temperatures with lower precursor pressures, as presented in Figure 3. The Si−C stretching vibration is observed around 780 cm^{-1}.[39,40,41]

Several peaks appear in the region 500−650 cm^{-1}. For example, there are two FTIR absorbance frequencies at the ranges 501−509 and 560−586 cm^{-1}. These peaks may be due to the symmetric and antisymmetric stretching vibrations of Si−Cl_2, which are observed as strong vibrations around 513 and 563 cm^{-1} on porous silicon exposed to SiH_2Cl_2.[42] The intensities of these peaks decrease with increasing substrate temperature. C−Cl vibrations typically occur between 505 and 760 cm^{-1}, but the peaks have not been assigned here.

3.5. EDXRF Measurements. FTIR detects chlorine atoms that are bound to the substrate or to the deposited film, i.e., to the silicon or carbon atoms. EDXRF spectroscopy is more sensitive than FTIR and yields information about the relative total chlorine concentration in films deposited at different temperatures. The detection limit of the EDXRF instrument is 0.1%.

The EDXRF measurements showed the total chlorine content of the films to decrease with increasing deposition temperature. When the substrate temperature was increased from 303 to 353 K, the amount of chlorine decreased to about one-third of its original value. Increasing the temperature further to 523 K produced films whose chlorine content was one-fifth that of films deposited at 303 K. Deposition at 573−593 K produced *a*-C films in which chlorine was still present but its concentration was very small.

Deposition at 643 K appeared to produce a chlorine-free *a*-C film on the quartz substrate. Some chlorine may still have been present on the silicon substrate, however. This result can be understood in terms of the relative numbers of silicon atoms present and capable of bonding to chlorine in the two substrates. As discussed above, the presence of some bonded chlorine on the silicon substrate is also suggested by the FTIR spectra (see Figure 3).

3.6. Surface Morphology. For detailed information on the surface morphology of the as-grown *a*-C films, the films were examined by atomic force microscopy (AFM). The AFM images reveal that the films deposited on quartz substrates are very smooth (see the RMS values given in Table 1). The films deposited at the lowest substrate temperatures were the smoothest (cf. Figures 4 and 5). The thickness of the films varied between ca. 200 and 700 nm.

The AFM images of the film grown on the silicon (111) substrate at 573 K with the highest laser power indicate a surface morphology not unlike the [111] texture of polycrystalline diamond (see Figure 6). According to the SAWS measurements, this film yielded the highest Young's modulus. Focusing of the laser beam at the same substrate temperature yielded softer films with smoother surfaces and without separate hillocks (Figure 7).

3.7. Optical Properties. The optical absorption characteristics of amorphous carbon films on the quartz substrates were investigated by photothermal deflection spectroscopy (PDS). The results are interpreted using the Tauc and Urbach theories.[11,43] Tauc plots, i.e. plots of $(\alpha E)^{1/2}$, where α is the optical absorption coefficient, versus the energy E of the photon absorbed by the

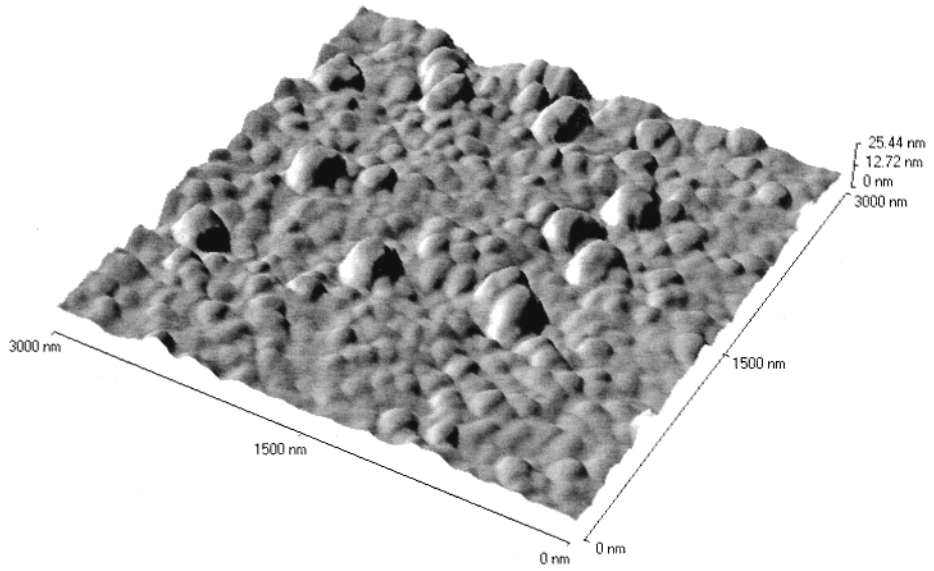

Figure 5. AFM image of an *a*-C:H,Cl film deposited on Si(111) at 518 K.

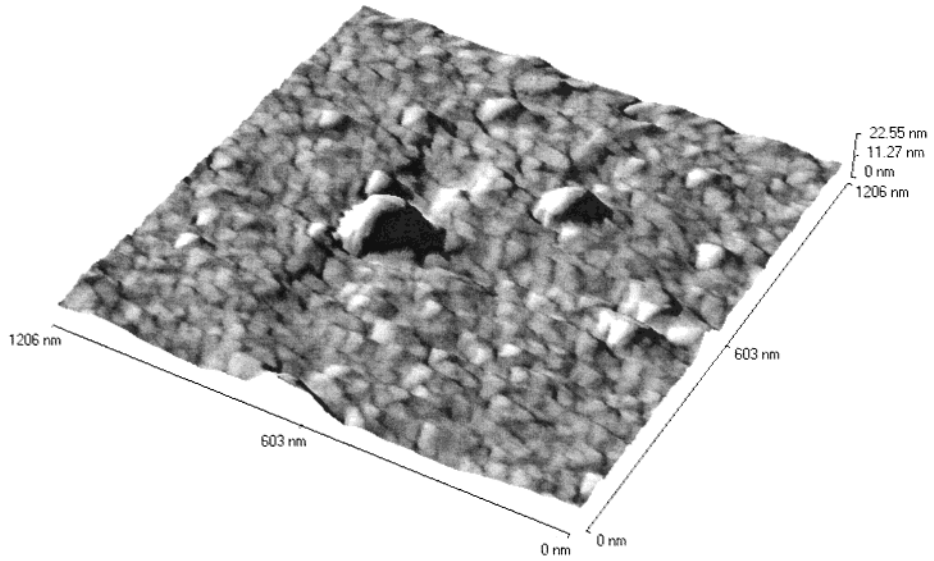

Figure 6. AFM image of an amorphous carbon film grown on the Si(111) substrate at 573 K.

film,[38] are presented in Figures 8 and 9 for amorphous carbon films deposited at two different CH_3Cl partial pressures. Neither the change of the CH_3Cl partial pressure nor the distance between the laser beam and the substrate surface appeared to influence the optical properties. The irrelevance of the laser beam−substrate distance may have been apparent only, as the distance adjustment on the instrument is at millimeter scale.

According to the Tauc plot relation $(\alpha E)^{1/2} = G(E - E_g)$, the intercept of the tangential extrapolation of the Tauc plot at $(\alpha E)^{1/2} = 0$ gives the Tauc optical energy gap (E_g), which is an estimate of the gap between the valence and conduction bands.[44] The tangents for the Tauc plots were calculated as least-squares fits at 10^4 cm^{-1} < α < 10^5 cm^{-1}, where the change of $(\alpha E)^{1/2}$ is directly proportional to E and the gradient G is constant. Table 1 shows the energies of the Tauc gaps compared with those of the E_{o4} gaps, i.e., the energies at which the optical absorption coefficient $\alpha = 10^4$ cm^{-1}.[38,44]

The E_{o4} gaps are ca. 0.3−0.5 eV larger than the Tauc gaps. Usually, the E_{o4} values are regarded as more reliable estimates of the optical energy gaps of amorphous carbon films, which have broad absorption edges. The optical Tauc gap decreases from 2.3 to 0.1 eV in the temperature range 303−623 K. The Tauc gaps, which give the lower limits for the optical gaps, are presented as a function of the deposition temperature in Figure 10.

The Urbach energy (E_o), which gives an estimate of the density of defect states at the band edge of the material, is obtained as the inverse slope of the Urbach tail. In many amorphous semiconductors, the Urbach tail is the lower part of the edge, i.e., where $\alpha < 10^4$ cm^{-1}. In this region, the absorption coefficient depends exponentially on the photon energy according to the relation $\alpha = \alpha_o \exp(E/E_o)$.

The calculated Urbach energies are collected in Table 1 and presented as a function of the deposition temperature in Figure 11. The Urbach energy increases from 240 meV to infinity in the temperature range 303−643 K. As can be seen, the values are more or less constant between 303 and 423 K and begin to rise when the deposition temperature is increased from 423 to 493 K. At the same time, the optical gap becomes narrower, decreasing from 1.6 to 1.0 eV. As was seen in the EDXRF measurements, the amount of chlorine decreases sharply in this same region. Chlorine atoms bound in amorphous carbon thin films deposited on silicon substrates appear to be slightly more stable against thermal desorption than chlorine atoms on

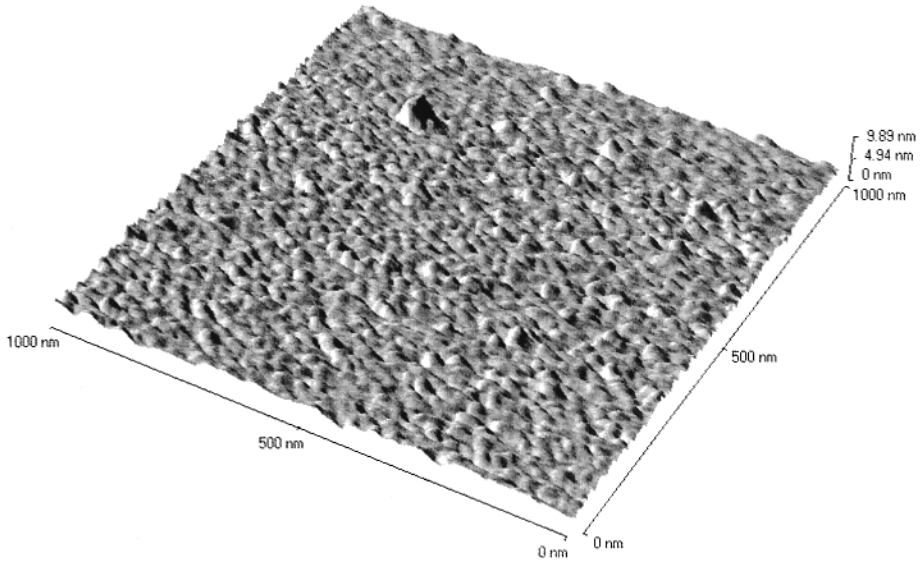

Figure 7. AFM image of the *a*-C film deposited on a quartz substrate at 573 K using a focused laser beam.

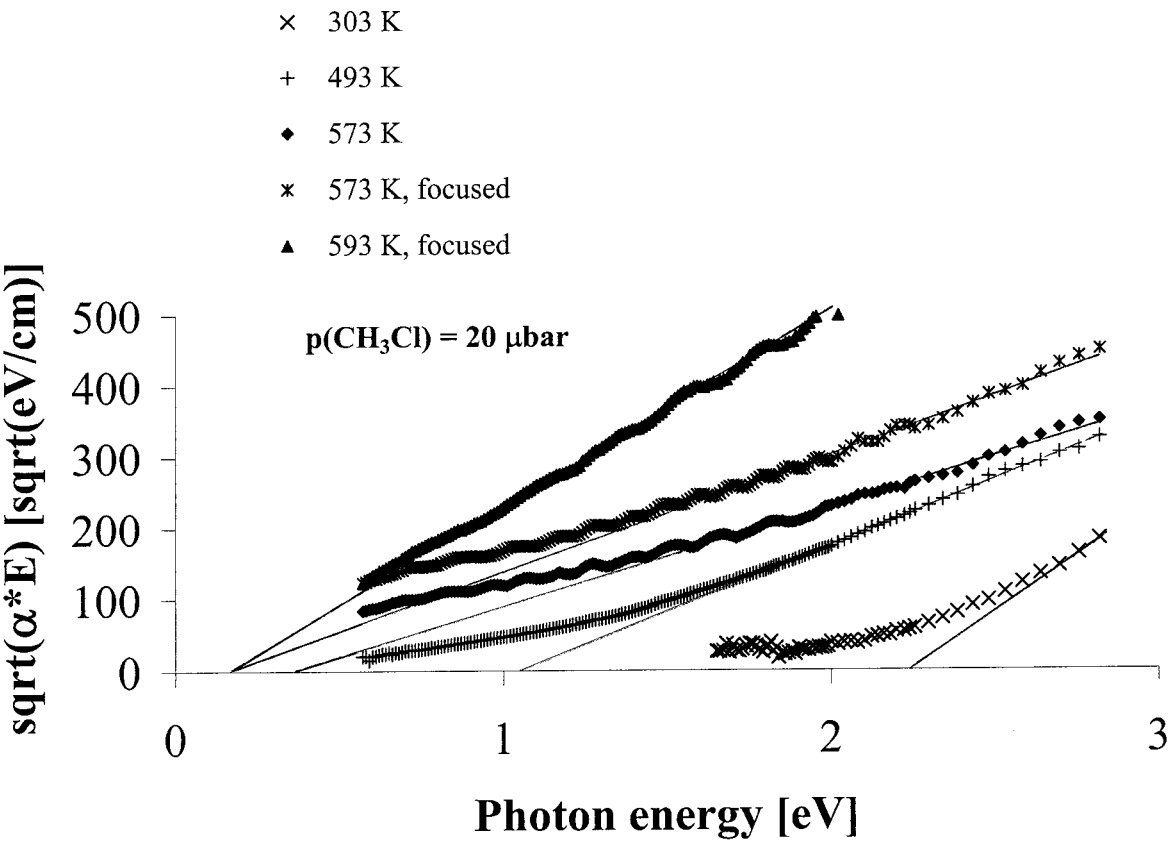

Figure 8. Tauc plots of amorphous carbon films deposited using a CH_3Cl partial pressure of 20 μbar.

crystalline diamond surfaces. On diamond surfaces exposed to atomic chlorine, the concentration of chlorine atoms decreases to virtually zero at 423 K.[45]

The Urbach energy increases further above 493 K (Figure 11) and starts to approach infinity, while the E_g value approaches zero at approximately 573 K. The increase in the number of defect states, together with the decrease in the gap and decrease in the chlorine content, indicates that the carbon network is adopting new structures. The films grown at 573 K were light brown in color.

When hydrogen is present in the deposition process, it could be possible that, in the temperature range in which dramatic changes are occurring in the optical properties of the deposited film, the amount of hydrogen is decreasing rapidly. In a halogen-free plasma deposition process producing hydrogenated tetrahedral amorphous carbon films, graphitization of the C−C bonds has been observed around 523 K.[18] In addition, in annealing studies on hydrogen-containing diamond-like carbon (*a*-C:H) films grown by chemical vapor deposition techniques, the diamond-like carbon network has been shown to begin to convert to nanocrystalline graphite above 573−673 K.[23,46] This conversion was associated with hydrogen evolution from the film. In the present work, however, the FTIR measurements showed that the concentration of hydrogen atoms in the films

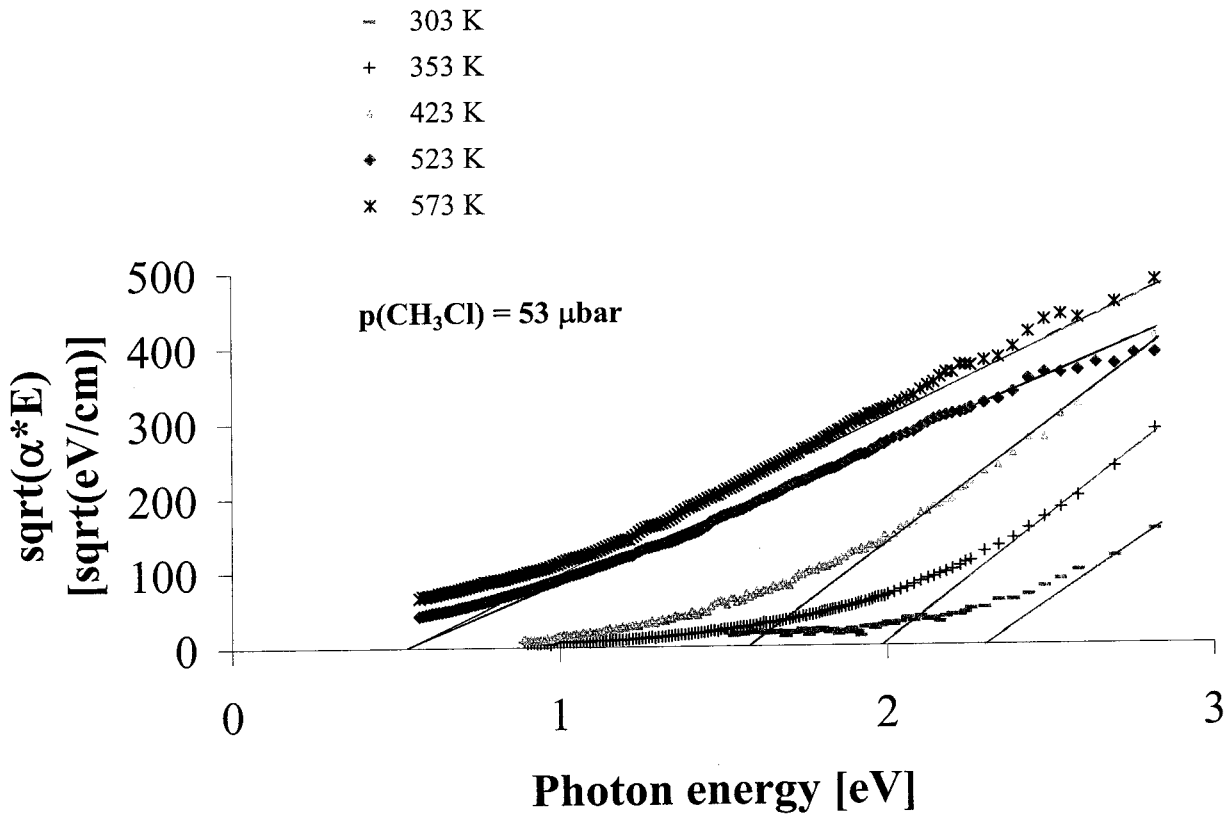

Figure 9. Tauc plots of amorphous carbon films grown with a CH_3Cl partial pressure of 53 μbar.

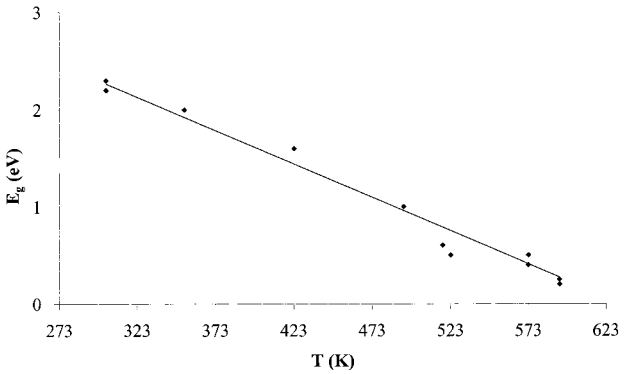

Figure 10. Tauc gaps as a function of the deposition temperature.

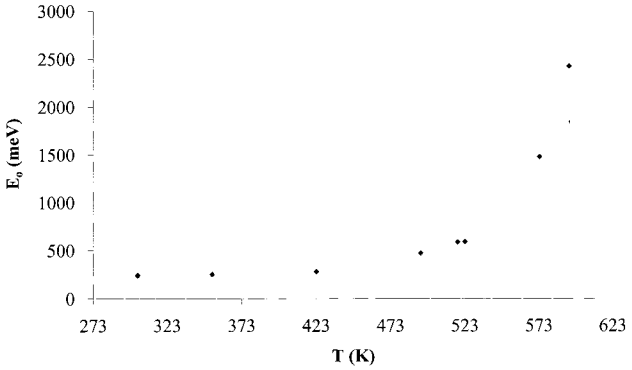

Figure 11. Urbach energies as a function of the deposition temperature.

deposited with low precursor pressures above 490 K was very small and probably smaller than the concentrations of chlorine atoms. Hence, the restructuring of the carbon network into a more graphitic structure, which starts at the lower deposition temperatures and becomes more clearly visible at higher temperatures, probably results from the decrease in the amount of covalently bonded chlorine atoms in the films.

According to the literature, the absorption edge of hydrogenated amorphous carbon films shifts toward lower energies as the substrate temperature is increased.[43] It has been concluded from this that the gap decreases when the sp^2 content of the film increases.[47] The effect of the hydrogen content on the optical gap and on the density of defect states[1] has been inferred to be only indirect. In our work, over the whole temperature range, not only the hydrogen content but also the chlorine content decreased when the deposition temperature was increased. The FTIR results show the intensities of the sp^2 vibration bands to increase when the substrate temperature increases. Evidently the gap of our *a*-C:H,Cl films is determined by the π and π^* states of the sp^2 sites in the carbon network, as in the case of the *a*-C:H and *a*-C films.[47]

In the hydrogenated amorphous carbon thin films considered suitable for electronic applications, band gaps wider than 2.0 eV and Urbach energies smaller than 250 meV are desirable.[48] In this work, the largest optical gap, 2.3 eV, and the lowest Urbach energy, 240 meV, measured in the films deposited at the lowest temperature (303 K), fulfill these requirements. These films were the most opaque and were almost colorless. The chlorine incorporated in the films evidently helps to stabilize the tetrahedral coordination (sp^3 bonding) and the transparency, as well as the band gaps, but it does not increase the hardness in the way the bonded hydrogen does. Although the films grown at room-temperature cannot, therefore, be used as hard coatings, they might be used to coat materials that suffer or deform at higher temperatures. In turn, the film grown at 573 K does not have as good optical properties, but according to the SAWS measurements, does have a high Young's modulus and might find use as a hard coating with selective transparency.

4. Conclusions

A VUV-laser-assisted chemical vapor deposition method was used to grow *a*-C films with low hydrogen contents from CH_3-Cl at low substrate temperatures. The films were characterized with a set of complementary methods.

The largest optical gap, 2.3 eV, and the lowest Urbach energy, 240 meV, were measured in the films deposited at the lowest temperature (303 K). These films were also the most opaque and were almost colorless. Incorporation of chlorine evidently helped to stabilize the tetrahedral coordination and transparency. One use for the films might be to coat materials that do not endure higher temperatures.

The chlorine concentration decreased as a function of the deposition temperature and was very low in the *a*-C:H,Cl films deposited at 523 and 573 K. As measured by SAW spectroscopy, the film deposited at 573 K on silicon with the F_2 laser tuned to its maximum power yielded the highest Young's modulus (180−200 GPa). The elastic properties of the films deposited with lower laser powers were worse.

According to the PDS measurements, the lower limit for the transition temperature for graphitization of the C−C bonds in the films is close to 493−518 K. As determined by EDXRFS, the number of chlorine atoms, which bond slightly more weakly to carbon atoms than does hydrogen, decreases significantly between 493 and 518 K. A relatively high degree of sp^2 bonding was observed in the FTIR spectra for samples deposited above this temperature range. This range falls slightly below the transition temperature of 523 K observed in hydrogenated tetrahedral amorphous carbon films produced by halogen-free plasma deposition. We conclude that the reduction in the chlorine concentration causes the carbon network to restructure into a more graphitic form.

Acknowledgment. T. I. Hukka gratefully acknowledges the financial support received from the Academy of Finland, the Alfred Kordelin Foundation in Finland, and Prof. Peter Hess at the University of Heidelberg in Germany. Mr. Ralph Kuschnereit is thanked for performing the SAWS measurements and Mr. Arndt Heerwagen for measuring the Raman spectra at the University of Heidelberg. In addition, Dr. Sirpa Peräniemi is thanked for running the EDXRFS spectra of the a-C films at the University of Joensuu, Finland. The work was carried out at the Institute of Physical Chemistry, University of Heidelberg, Im Neuenheimer Feld 253, D-69120 Heidelberg, Germany.

References and Notes

(1) Amaratunga, G. A. J.; Robertson, J.; Veerasamy, V. S.; Milne, W. I.; McKenzie, D. R. *Diamond Relat. Mater.* **1995**, *4*, 637.

(2) Patterson, D. E.; Chu, C. J.; Bai, B. J.; Xiao, Z. L.; Komplin, N. J.; Hauge, R. H.; Margrave, J. L. *Diamond Relat. Mater.* **1992**, *1*, 768.

(3) See also the references in: (a) Hukka, T. I.; Rawles, R. E.; D'Evelyn, M. P. *Thin Solid Films* **1993**, *225*, 212. (b) Hukka, T. I.; Pakkanen, T. A.; D'Evelyn, M. P. *J. Phys. Chem.* **1995**, *99*, 4710. (c) Hukka, T. I.; Pakkanen, T. A.; D'Evelyn, M. P. *Surf. Sci.* **1996**, *359*, 213.

(4) Stenberg, G.; Piglmayer, K.; Boman, M.; Carlsson, J.-O. *Appl. Surf. Sci.* **1997**, *109/110*, 549.

(5) Molian, P. A.; Janvrin, B.; Molian, A. M. *Wear* **1993**, *165*, 133.

(6) Toshinori, Y.; Yoshiyuaki, G.; Haruhiko, N. *Jpn. Kokai Tokkyo Koho*, Patent JP63028864, 1988.

(7) Ong, H. C.; Chang, R. P. H. *Phys. Rev. B* **1997**, *55*, 13213.

(8) Chuang, F. Y; Sun, C. Y.; Cheng, H. F.; Huang, C. M.; Lin, I. N. *Appl. Phys. Lett.* **1996**, *68*, 1666 and references therein.

(9) Karstens, H.; Knobloch, J.; Winkler, A.; Pusel, A.; Barth, M.; Hess, P. *Appl. Surf. Sci.* **1995**, *86*, 521.

(10) Lee, L. C.; Suto, M. *Chem. Phys.* **1987**, *114*, 423.

(11) Matsumi, Y.; Tonokura, K.; Kawasaki, M.; Inoue, G.; Satyapal, S.; Bersohn, R. *J. Chem. Phys.* **1991**, *94*, 2669.

(12) Pusel, A. M. *Photothermische Deflexions-Spektroskopie an amorphen wasserstoffhaltigen Halbleitern*. Die Diplomarbeit, Fakultät fuer Physik und Astronomie, Ruprecht-Karls-Universität Heidelberg, Germany, 1993, and references therein.

(13) Kuschnereit, R.; Hess, P.; Albert, D.; Kulisch, W. *Thin Solid Films* **1998**, *312*, 66.

(14) Pharr, G. M.; Callahan, D. L.; McAdams, S. D.; Tsui, T. Y.; Anders, S.; Anders, A.; Ager, J. W., III; Brown, I. G.; Bhatia, C. S.; Silva, S. R. P.; Robertson, J. *Appl. Phys. Lett.* **1996**, *68*, 779.

(15) Tsai, H.; Bogy, D. B. *J. Vac. Sci. Technol. A* **1987**, *5*, 3287.

(16) Sattel, S.; Weiler, M.; Gerber, J.; Giessen, T.; Roth, H.; Scheib, M.; Jung, K.; Ehrhardt, H.; Robertson, J. *Diamond Relat. Mater.* **1995**, *4*, 333.

(17) Tamaki, K.; Nakamura, Y.; Watanabe, Y.; Hirayama, S. *J. Mater. Res.* **1995**, *10*, 431.

(18) Sattel, S.; Robertson, J.; Ehrhardt, H. *J. Appl. Phys.* **1997**, *82*, 4566.

(19) Knight, D. S.; White, W. B. *J. Mater. Res.* **1989**, *4*, 385.

(20) McKenzie, D. R. *Rep. Prog. Phys.* **1996**, *59*, 1611.

(21) Dischler, B.; Bubenzer, A.; Koidl, P. *Solid State Commun.* **1983**, *48*, 105.

(22) Friedman, T. A.; McCarty, K. F.; Barbour, J. C.; Siegal, M. P.; Dibble, D. C. *Appl. Phys. Lett.* **1996**, *68*, 1643.

(23) Tallant, D. R.; Parmeter, J. E.; Siegal, M. P.; Simpson, R. L. *Diamond Relat. Mater.* **1995**, *4*, 191.

(24) Wagner, J.; Wild, C.; Koidl, P. *Appl. Phys. Lett.* **1991**, *59*, 779.

(25) Gerber, J.; Weiler, M.; Sohr, O.; Jung, K.; Ehrhardt, H. *Diamond Relat. Mater.* **1994**, *3*, 506.

(26) Nemanich, R. J.; Glass, T. J.; Lucovsky, G.; Scroder, R. E. *J. Vac. Sci. Technol. A* **1988**, *6*, 1783.

(27) Schwan, J.; Ulrich, S.; Roth, H.; Ehrhardt, H.; Silva, S. R. P.; Robertson, J.; Samlenski, R.; Brenn, R. *J. Appl. Phys.* **1996**, *79*, 1416.

(28) Fayette, L.; Marcus, B.; Mermoux, M.; Rosman, N.; Abello, L.; Lucazeau, G. *J. Mater. Res.* **1997**, *12*, 2689.

(29) Lee, J.; Collins, R. W.; Messier, R.; Strausser, Y. E. *Appl. Phys. Lett.* **1997**, *70*, 1527.

(30) Erz, R.; Dötter, W.; Jung, K.; Ehrhardt, H. *Diamond Relat. Mater.* **1995**, *4*, 469.

(31) McNamara Rutledge, K.; Gleason, K. K. *Chem. Vap. Deposition* **1996**, *2*, 37 and references therein.

(32) Dischler, B.; Bubenzer, A.; Koidl, P. *Appl. Phys. Lett.* **1983**, *42*, 636.

(33) Walters, J. K.; Newport, R. J.; Parker, S. F.; Howells, W. S.; Bushnell-Wye, G *J. Phys.: Condens. Matter* **1998**, *10*, 4161.

(34) Grill, A.; Patel, V. *Appl. Phys. Lett.* **1992**, *60*, 2089.

(35) Lukins, P. B.; McKenzie, D. R.; Vassallo, A. M.; Hanna, J. V. *Carbon* **1993**, *31*, 569.

(36) Gonzalez-Hernandez, J.; Chao, B. S.; Pawlik, D. A. *J. Vac. Sci. Technol. A* **1989**, *7*, 2332.

(37) Stenzel, O.; Schaarschmidt, G.; Wolf, F.; Vogel, M.; Wallendorf, T. *Thin Solid Films* **1991**, *203*, 11.

(38) Robertson, J. *Adv. Phys.* **1986**, *35*, 317.

(39) Herlin, N.; Lefebvre, M.; Péalat, M.; Perrin, J. *J. Phys. Chem.* **1992**, *96*, 7063.

(40) Fölsch, J.; Ruebel, H.; Schade, H. *Appl. Phys. Lett.* **1992**, *61*, 3029.

(41) John, P.; Graham, C.; Milne, D. K.; Jubber, M. G.; Wilson, J. I. B. *Diamond Relat. Mater.* **1996**, *5*, 256.

(42) Robinson, M. B.; Dillon, A. C.; George, S. M. *J. Vac. Sci. Technol. A* **1995**, *13*, 35.

(43) Anderson, D. A. *Philos. Mag.* **1977**, *35*, 17.

(44) Weiler, M.; Sattel, S.; Giessen, T.; Jung, K.; Ehrhardt, H.; Veersamy, V. S.; Robertson, J. *Phys. Rev. B* **1996**, *53*, 1594.

(45) Freedman, A. *J. Appl. Phys.* **1994**, *75*, 3112.

(46) Causey, R. A.; Wampler, W. R.; Walsh, D. *J. Nucl. Mater.* **1990**, *176/177*, 987.

(47) Robertson, J.; O'Reilly, E. P. *Phys. Rev. B* **1987**, *35*, 2946.

(48) Hess, P. *Electronic Materials Chemistry*; Pogge H. B., Ed.; Marcel Dekker, Inc.: New York, 1996; Chapter 4.